remote sensing

MDPI

Article

Disaggregation of SMOS Soil Moisture to 100 m Resolution Using MODIS Optical/Thermal and Sentinel-1 Radar Data: Evaluation over a Bare Soil Site in Morocco

Omar Ali Eweys [1,2,3,*], Maria José Escorihuela [1], Josep M. Villar [2], Salah Er-Raki [4], Abdelhakim Amazirh [4,6], Luis Olivera [6], Lionel Jarlan [6], Saïd Khabba [5] and Olivier Merlin [5,6]

1 isardSAT, ParcTecnològic Barcelona Activa, Carrer de Marie Curie, 8, 08042 Barcelona, Spain; mj.escorihuela@isardsat.cat
2 Environment and Soil Science Department, University of Lleida, 25003 Lleida, Spain; jmvillar@macs.udl.cat
3 Soil Sciences Department, Faculty of Agriculture, Cairo University, Gamaa Street 6, 12613 Giza, Egypt;
4 LP2M2E, Dèpartment de Physique Appliquèe, Facultè des Sciences et Techniques, Universitè Cadi Ayyad, 40000 Marrakech, Morocco; s.erraki@uca.ma (S.E.-R.); abdelhakim.amazirh@gmail.com (A.A.)
5 LMME, Dèpartment de Physique, Facultè des Sciences Semlalia, Universitè Cadi Ayyad, 40000 Marrakech, Morocco; khabba@uca.ma (S.K.); olivier.merlin@cesbio.cnes.fr (O.M.)
6 CESBIO, Université de Toulouse, IRD, UPS, CNRS, CNES, 31400 Toulouse, France; olivera-guerrale@cesbio.cnes.fr (L.O.); lionel.jarlan@cesbio.cnes.fr (L.J.)
* Correspondence: omar.ahmed@agr.cu.edu.eg

Received: 28 September 2017; Accepted: 7 November 2017; Published: 10 November 2017

Abstract: The 40 km resolution SMOS (Soil Moisture and Ocean Salinity) soil moisture, previously disaggregated at a 1 km resolution using the DISPATCH (DISaggregation based on Physical And Theoretical scale CHange) method based on MODIS optical/thermal data, is further disaggregated to 100 m resolution using Sentinel-1 backscattering coefficient (σ°). For this purpose, three distinct radar-based disaggregation methods are tested by linking the spatio-temporal variability of σ° and soil moisture data at the 1 km and 100 m resolution. The three methods are: (1) the weight method, which estimates soil moisture at 100 m resolution at a certain time as a function of σ° ratio (100 m to 1 km resolution) and the 1 km DISPATCH products of the same time; (2) the regression method which estimates soil moisture as a function of σ° where the regression parameters (e.g., intercept and slope) vary in space and time; and (3) the Cumulative Distribution Function (CDF) method, which estimates 100 m resolution soil moisture from the cumulative probability of 100 m resolution backscatter and the maximum to minimum 1 km resolution (DISPATCH) soil moisture difference. In each case, disaggregation results are evaluated against in situ measurements collected between 1 January 2016 and 11 October 2016 over a bare soil site in central Morocco. The determination coefficient (R^2) between 1 km resolution DISPATCH and localized in situ soil moisture is 0.31. The regression and CDF methods have marginal effect on improving the DISPATCH accuracy at the station scale with a R^2 between remotely sensed and in situ soil moisture of 0.29 and 0.34, respectively. By contrast, the weight method significantly improves the correlation between remotely sensed and in situ soil moisture with a R^2 of 0.52. Likewise, the soil moisture estimates show low root mean square difference with in situ measurements (RMSD = 0.032 m^3 m^{-3}).

Keywords: soil moisture and ocean salinity satellite (SMOS); DISPATCH; radar; Sentinel-1; disaggregation; soil moisture

1. Introduction

Soil moisture (sm) is a land state variable governing the interaction between the land surface and atmosphere through playing its role in various components of the water and energy cycle, such as evapotranspiration, groundwater recharge, and surface runoff. Thus, comprehensive monitoring programs providing high quality soil moisture information are needed for precisely modeling the exchange of water, energy, and carbon fluxes between land and atmosphere. Given that in situ measurements are labor intensive, site specific and represent tiny soil fractions, remotely sensed imagery is a unique alternative for providing frequent soil moisture estimates at integrated spatial scales, which can also be used for augmenting sparsely distributed measurements [1]. The high sensitivity of microwave imagery to soil moisture and its ability to work under all weather conditions make it a suitable candidate for capturing the spatial and temporal variability of soil moisture [2]. In particular, L-band radiometry is favorable due to an optimal signal to noise ratio [3,4]. The Soil Moisture and Ocean Salinity (SMOS) mission, launched in November 2009, utilizes an L-band interferometric radiometer for providing topsoil (3–5 cm) moisture maps at 30–55 km resolution [5,6]. Although, SMOS soil moisture products have been regularly validated [7,8] and evaluated as appropriate for hydro-climate applications [9], higher spatial resolutions detailing the soil moisture distribution within the passive microwave pixel is highly required, especially for agricultural applications [10].

A range of disaggregation methods of coarse resolution passive microwave-based soil moisture products rely on active microwave observations acquired at high (several tens of meters) resolution by synthetic aperture radars (SAR) [10]. Chauhan et al. [11] and O'Neill et al. [12] showed that physically-based radiative transfer modeling approaches can be used for exploiting potential synergy between active and passive observations within the context of data disaggregation. Statistical and hydrological models were also vastly used to describe the temporal and spatial characteristics of soil moisture within catchments [10,13–16]. Other approaches based on the change detection technique were developed. For instance, Njoku et al. [1] retrieved soil moisture by applying an approach based on the change detection on passive/active L-band system data acquired during the Southern Great Plains Experiment in 1999. The algorithm was further matured by Piles et al. [17] through using an observation system simulation experiment, which led to provide absolute values of moisture content. In the same vein, Das et al. [18] improved the change detection algorithm for providing absolute values of soil moisture, which resulted in developing the baseline algorithm for Soil Moisture Active and Passive mission (SMAP) combined active/passive soil moisture product. The baseline algorithm was then modified [19] for overcoming the disadvantage of being highly dependent on the accuracy of the retrieved passive microwave soil moisture [10].

Alternatively, optical/thermal observations, especially the 1 km resolution MODIS (MODerate resolution Imaging Spectroradiometer) data, have been widely used for disaggregation of SMOS like soil moisture data. In general, an assumed relationship between land surface temperature (LST), normalized difference vegetation index (NDVI) and near-surface soil moisture is employed for disaggregation [9] based on the triangle [20,21] or trapezoid [22] approaches [10]. Such a relationship can be described in a regression form specific to the surface conditions encountered over the study region at the time of satellite overpass. The link between LST and near-surface soil moisture can also be formalized more physically using an evaporation model as it is done in the DISPATCH (DISaggregation based on Physical And Theoretical scale Change) method [23,24].

In general, the combination of multi-source data is recommended for disaggregating SMOS data to finer resolutions, especially when using data acquired over a swath width (for instance 185 km for Landsat and 60 km for ASTER, Advanced Scanning Thermal Emission and Reflection Radiometer) much narrower than that (~1000 km) of SMOS. Merlin et al. [25] used MODIS and ASTER data for sequentially disaggregating SMOS product to 4 km resolution (using MODIS) and 500 m (using ASTER) resolution. The results showed that using an intermediate resolution of 4 km led to improved results than when ASTER was used for disaggregating SMOS directly to the targeted (500 m) resolution.

That is notably because MODIS reduced the non-linearity influences across scales between the soil evaporation rate and soil moisture [23].

Note that the temporal resolution of the observations used for disaggregation is of great importance for providing disaggregated soil moisture at suitable time intervals. Since MODIS data are available twice a day, the availability (on clear sky days) of the 1 km resolution DISPATCH product over time depends solely on the SMOS revisit time, which is three days. ASTER and Landsat data can be used for disaggregating the 1 km DISPATCH products to finer resolution [23,25]. However, the availability of ASTER and Landsat data over time (16 days) makes the use of the disaggregated soil moisture in agriculture questionable. In fact, more frequent (few days) disaggregated soil moisture estimates are required in order to monitor the water availability for plants and, hence, to schedule the time and water amount of irrigation [26]. The C-band backscatter data acquired by the synthetic aperture radar (SAR) sensor aboard Sentinel-1 satellite is a potential candidate for disaggregating the 1 km DISPATCH products to 100 m resolution due to the shorter revisit time and the free availability to public users.

In this context, this work aims at employing the C-SAR data acquired every six days by Sentinel-1 for disaggregating SMOS products to 100 m resolution using the 1 km DISPATCH product as a reference at an intermediate resolution. In this work, three different methods are investigated: (1) the 100 m to 1 km resolution backscatter ratio is used as an indicator for soil moisture spatial variability; (2) the regression form of the near linear relationship between soil moisture and backscatter is used for disaggregation; and (3) the cumulative probability (CDF) of the backscatter is used for estimate 100 m resolution soil moisture given the maximum and minimum soil moisture difference captured by the 1 km DISPATCH product. Given that vegetation characteristics (water content and structure) influence C-SAR data, the three methods are inter-compared over a bare soil site as a first step before more generic approaches could be developed in the future. The three methods are evaluated against in situ measurements in terms of mean, bias, coefficient of determination (R^2), root mean square difference (RMSD) and mean absolute difference (MAD).

2. Study Area and Data Sets

2.1. Study Area

Figure 1a shows the study area known as Sidi Rahal site which is 5 km^2 located 60 km east of Marrakesh city, Morocco (31°40′27.06″–31°43′9.06″N, 7°20′0.76″–7°22′42.76″W). Figure 1b is a land use map for the study area showing that the main uses are trees, bare soil and agricultural fields in addition to urban area. Based on the Köppen climate classification [27], the area is characterized by Mediterranean semi-arid climate with an average annual rainfall of 250 mm. The terrain is flat with elevation of 550 m above sea level and. The agricultural fields remained under bare soil conditions between 1 January 2016 and 1 November 2016 [28].

2.2. DISPATCH Soil Moisture Product

DISPATCH soil moisture maps were produced over the study area for the period between 1 January 2016 and 11 October 2016. The SMOS level-3 soil moisture data were disaggregated to 1 km resolution using the new SMOS level-4 processor (C4DIS) developed as part of the French ground segment for SMOS level-3 and level-4 data (Centre Aval de Traitment des Donnees SMOS). Details about the C4DIS processor and product can be found in Molero et al. [29]. Briefly, the C4DIS processor implements the DISPATCH method [23,24,30] at the quasi global scale for each selected MODIS tile separately. The DISPATCH method expresses the 1 km resolution soil moisture as a function of the ~40 km resolution SMOS level-3 soil moisture and the soil evaporation efficiency estimated at 1 km resolution from MODIS LST and NDVI data.

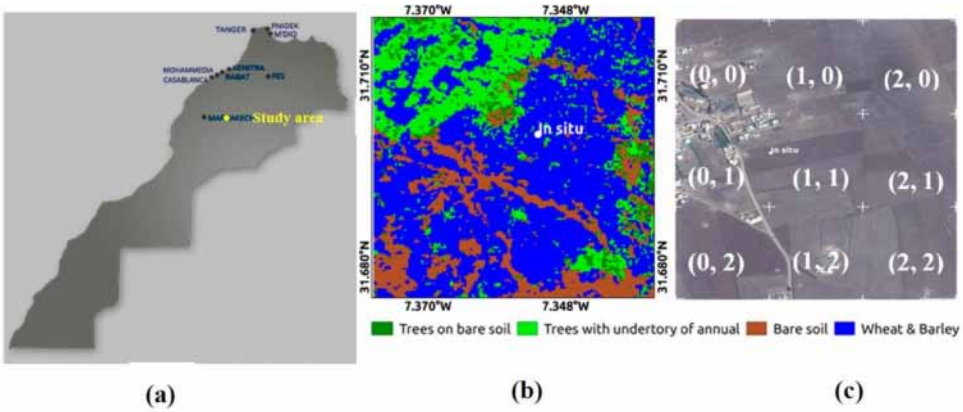

Figure 1. (**a**) The study area located at the east of Marrakech city, Morocco; (**b**) land cover/land use map of the study area (5 km^2); and (**c**) Google map of nine pixels (100 m resolution) of the study area where pixel (1, 1) includes the station for the in situ measurements.

2.3. SAR Data

Forty-six level-1 Ground Range Detected (GRD) C-band SAR scenes acquired by Sentinel-1 between 1 January 2016 and 11 October 2016 in ascending pass direction at a nominal time of 18:33 UTC are employed for this study. Note that the descending pass direction never matches the DISPATCH product over the study area. Sentinel-1 has four operating modes; however, over land, it is nominally in the interferometric wide swath (IW) mode and measures at dual (VV and VH) polarization with a 250 km swath at a 5 m by 20 m spatial resolution. The VH data are not used for this study since a significantly better correlation between radar and in situ soil moisture was found for VV than for VH over the study area [28]. However, the VH data can be employed for quantifying the vegetation contribution to the backscatter acquired by the satellite since VH is more sensitive to the vegetation properties [31].

2.4. In Situ Measurements

The Sidi Rahal site was equipped by a monitoring station (Figure 1b,c) in December 2013 in the frame work of the Joint International Laboratory TREMA (a French acronym for Remote Sensing and Water Resources in the Semi-Arid Mediterranean [32,33]. The monitoring station includes: (1) micro-meteorological instruments for estimating the latent and sensible heat fluxes at the soil–vegetation–atmosphere interface; (2) sensors for measuring rainfall, global radiation, temperature, relative humidity, and wind speed at a half-hourly time step; and (3) probes for measuring soil water content at different depths and at the time interval of 30 min. For this study, only the in situ measurements of the topsoil (5 cm) moisture content are used. Data were extracted on the 28 dates when both DISPATCH and C-SAR Sentinel-1 data were available.

3. Methodology

Processing the C-band SAR data is an essential step before applying the proposed methods. In particular, the data processing consisted of:(1) converting radar reflectivity into physical units (calibration); (2) reducing the spatial resolution by producing square pixels to improve the radiometric resolution (noise reduction); (3) using a median filter of a 7 by 7 window to alleviate the speckle effect (speckle filtering); and (4) converting the data from ground range geometry to backscatter using the Shuttle Radar Topography Mission (SRTM) 30 m digital elevation model (terrain correction).

It is worth mentioning that regions covered by evergreen trees were employed for testing various speckle filters since the backscatter show temporal stability over these trees. The median filter resulted in the most stable backscatter over time and, hence, it was selected for alleviating speckle in this study.

The above processing steps can be performed using the Sentinel Application Platform (SNAP) [34].

The vertical polarized backscatter noted σ° is first aggregated to 100 m and 1 km resolutions, and then normalized to vary between 0 and 1 for each i 1 km pixel and each j 100 m pixel, respectively. Formally, the normalized 1 km resolution σ° at pixel i and date t is defined as:

$$\sigma^\circ{}_{1\mathrm{km},i,t} = \frac{\sigma^\circ{}_{i,t} - \sigma^\circ{}_{min,\,i}}{\sigma^\circ{}_{max,\,i} - \sigma^\circ{}_{min,\,i}} \quad (1)$$

where $\sigma^\circ{}_{1\mathrm{km},i,t}$ is the normalized backscatter calculated from the backscatter σ° observed at time t and aggregated at the 1 km pixel i while max and min stand respectively for the maximum and minimum backscatter values reached at pixel i over the considered time series. Similarly, the normalized 100 m resolution σ° at pixel j and date t is defined as:

$$\sigma^\circ{}_{100\mathrm{m},j,t} = \frac{\sigma^\circ{}_{j,t} - \sigma^\circ{}_{min,j}}{\sigma^\circ{}_{max,\,j} - \sigma^\circ{}_{min,j}} \quad (2)$$

where $\sigma^\circ{}_{100\mathrm{m},j,t}$ is the normalized backscatter calculated from the backscatter σ° observed at time t and aggregated at the 100 m pixel j while max and min stand, respectively, for the maximum and minimum backscatter values reached at pixel j over the considered time series.

The following subsections along with Figure 2 describe the three applied methods for disaggregating the 1 km DISPATCH product to a resolution of 100 m using Sentinel-1data. The radar backscatter acquired over bare soil is a complex function of the sensor parameters (frequency, polarization and incidence angle) and the dielectric and geometric properties of the soil represented by soil moisture and surface roughness, respectively [2,35]. The sensor parameters are always known while intensive measurements are required for characterizing soil roughness due to its variable nature over space and time. However, Alvarez-Mozos et al. [36] and Baghdadi et al. [37] argued that soil roughness can be considered as a single scale stationary random process. Therefore, the variability in space and time of moisture content of bare soil can be, respectively, linked to the spatial and temporal patterns of the acquired backscatter. Various studies show the existence of a near linear relationship between sm and σ° over bare soils [38,39] which is addressed by:

$$\sigma^\circ{}_{100\mathrm{m},j,t} = P1_{j,t} \times sm_{j,t}^{P2_{j,t}} + P3_{j,t} \quad (3)$$

with P_1, P_2 and P_3 being parameters that are variable in space (j) and time (t) [40].

The three proposed radar-based disaggregation methods are mainly based on the quasi-linear relationship between sm and σ° (Equation (3) with P_2 close to (1)) where sm is estimated as a function of σ°. In particular, estimating soil moisture is controlled by the backscatter variability in: (1) space; (2) time; or (3) space and time. In general, Table 1 briefly compares the main assumption of each disaggregation method while detailed descriptions are provided in the following subsections.

Table 1. Main assumptions of the applied methods for disaggregating the 1 km DISPATCH product to 100 m resolution.

Method	Assumption
Weight	100 m resolution radar backscatter and soil moisture are related within a 1 km pixel and for a given date.
Regression	Parameters (e.g., intercept and slope) controlling the temporal relationship between radar backscatter and soil moisture are variable in space only (not in time).
CDF	The cumulative distribution function controls the temporal relationship between radar backscatter and soil moisture and varies in space only.

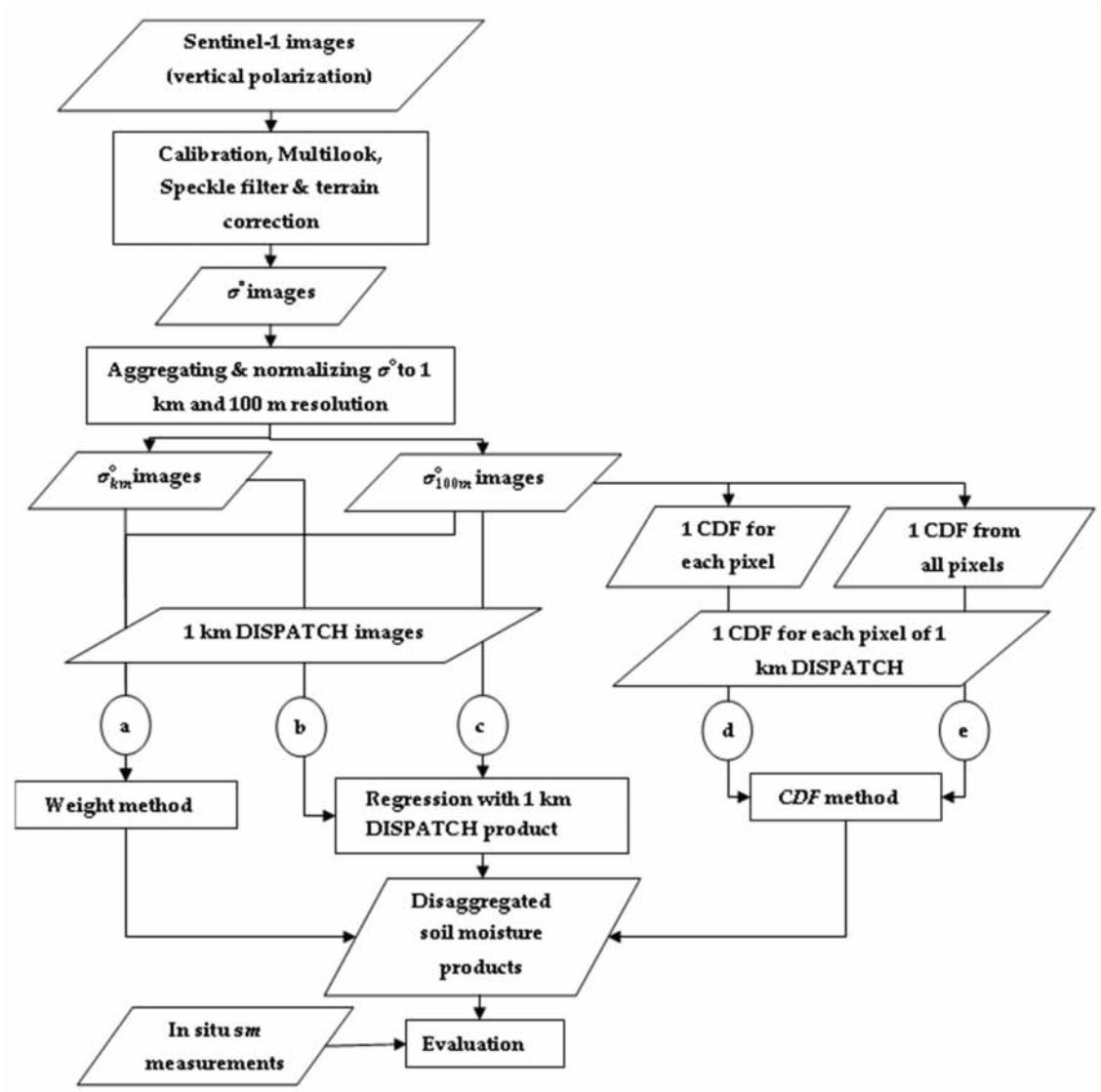

Figure 2. Disaggregating the 1 km DISPATCH product to 100 m resolution with methods referred to as: (**a**) weight; (**b**) $\text{regress}_{\text{km}}$; (**c**) $\text{regress}_{\text{100m}}$; (**d**) $\text{CDF}_{\text{every}}$; and (**e**) CDF_{all}.

3.1. Weight Method

For the weight method depicted by Figure 2a, we assume that the relative variabilities within 1 km pixels of 100 m resolution *sm* and 100 m resolution σ° are the same [41], meaning that:

$$\frac{sm_{100\text{m},j,t} - sm_{1\text{km},i,t}}{sm_{1\text{km},i,t}} = \frac{\overset{\circ}{\sigma}_{100\text{m},j,t} - \overset{\circ}{\sigma}_{1\text{km},i,t}}{\overset{\circ}{\sigma}_{1\text{km},i,t}} \quad (4)$$

Hence, the 100 m resolution *sm* disaggregated by the weight method can be written as:

$$sm_{100\text{m},j,t} = sm_{1\text{km},i,t} \times \frac{\overset{\circ}{\sigma}_{100\text{m},j,t}}{\overset{\circ}{\sigma}_{1\text{km},i,t}} \quad (5)$$

where *j* refers to the location of the 100 m resolution pixel within the *i* 1 km resolution DISPATCH pixel.

3.2. Regression Method

The second radar-based disaggregation approach employed in this study rests on finding the parameters describing the near-linear relation between soil moisture and backscatter (Equation (3)). By assuming that such a relationship is scale-invariant across the 100 m to 1 km scales, the 100 m resolution parameters are estimated by deriving the best fit between the 1 km resolution backscatter and DISPATCH *sm* data. Thus, the parameters of Equation (3) become variable in space (at the 1 km resolution) only. The best fit can be constructed in two distinct ways. The first, which is referred to as $\text{regress}_{\text{km}}$ and addressed by Equation (6), employs the time series of the 1 km DISPATCH product and the time series of the backscatter aggregated to 1 km resolution (Figure 2b). For each 1 km resolution pixel, the obtained parameters are used at 100 m resolution to construct the relation between 100 m resolution backscatter and soil moisture (Equation (7)). Hence, Equation (7) is reformed to Equation (8) to calculate the 100 m resolution disaggregated sm. The second referred to as $\text{regress}_{100\text{m}}$ and represented by Equation (9) employs the time series of the 1 km DISPATCH product and the time series of the backscatter aggregated to 100 m resolution. In particular, each pixel of the 1 km DISPATCH product is correlated to the corresponding 100 m resolution backscatter (Figure 2c). In return, an ensemble of 100 parameter sets is obtained within each 1 km DISPATCH pixel. For each ensemble, values of each parameter are averaged as shown by Equation (10) which is reformed to calculate the 100 m resolution disaggregated *sm* as expressed in Equation (11).

$$\overset{\circ}{\sigma}_{1\text{km},i} = P1_i \times sm_{1\text{km},\,i}^{P2_i} + P3_i \tag{6}$$

$$\overset{\circ}{\sigma}_{100\text{m},j} = P1_i \times sm_{100\text{m},j}^{P2_i} + P3_i \tag{7}$$

$$sm_{100\text{m},j} = \sqrt[P2_i]{\frac{\overset{\circ}{\sigma}_{100\text{m},j} - P3_i}{P1_i}} \tag{8}$$

$$\overset{\circ}{\sigma}_{100\text{m},j} = P1_j \times sm_{\text{km},i}^{P2_j} + P3_j \tag{9}$$

$$\overset{\circ}{\sigma}_{100\text{m},j} = P1_{j,mean} \times sm_{\text{km},i}^{P2_{j,mean}} + P3_{j,mean} \tag{10}$$

$$sm_{100\text{m},j} = \sqrt[P2_{j,mean}]{\frac{\overset{\circ}{\sigma}_{100\text{m},j} - P3_{j,mean}}{P1_{j,mean}}} \tag{11}$$

where mean refers to the arithmetic mean in case of averaging the parameters P_1, P_2, and P_3 of the 100 m resolution pixels within each 1 km DISPATCH pixel.

3.3. Cumulative Distribution Function (CDF) Method

Tomer et al. [40] and Eweys et al. [31] proposed an approach for transforming the near linear relation between backscatter and *sm* into a linear function based on the cumulative distribution function (CDF). In particular, the CDF transformation of a long time series of backscatter results in values ranging between 0 and 1, corresponding to the minimum and maximum soil moisture respectively. The relative soil moisture at any location at a certain time is hence considered as a function of the cumulative probability of the backscatter acquired over the same location and at the same time. Equation (11) was revealed by Tomer et al. [40] for retrieving *sm* based on the CDF of the backscatter:

$$sm_{i,t} = sm_{min,i} + (sm_{max,i} - sm_{min,i}) \times F\left(\overset{\circ}{\sigma}_{i,t}\right) \tag{12}$$

where $sm_{min,i}$, $sm_{max,i}$ and $F\left(\overset{\circ}{\sigma}_{i,t}\right)$ refer, respectively, to the minimum and maximum soil moisture at i DISPATCH pixel during a given period, and the cumulative probability of the backscatter acquired at

pixel i and time t. Note that Tomer et al. [40] considered field capacity and wilting point as maximum and minimum soil moisture, respectively.

Ranking radar backscatter time series acquired at a certain location (i or j) is an essential step for constructing the CDF. In particular, the backscatter values are ranked in an ascending order where each value is assigned a serial rank number (r) ranging from 1 to n (number of signals). Subsequently, the probability (P) is determined for each backscatter through applying the Equation (12) (Weibull method, cited by Raes [42]).

$$P = \frac{r}{(n+1)}100 \tag{13}$$

This study tests Tomer et al. [40] and Eweys et al. [31] approach for disaggregating the 1 km DISPATCH product to 100 m resolution using Sentinel-1 data, where the maximum and minimum soil moisture ($sm_{1\text{km},max,i}$ and $sm_{1\text{km},min,i}$, respectively) are estimated from the time series of DISPATCH data. To that end, the CDF of the backscatter is built in two distinct ways. The first method, known hereinafter as CDF_{all}, builds a single CDF from the 100 time series of 100 m resolution backscatter corresponding to each 1 km DISPATCH pixel (Figure 2d). The second method, known hereunder as $\text{CDF}_{\text{every}}$, builds a backscatter CDF for each 100 m resolution pixel. Thus, 100 distinct backscatter CDFs are built for each 1 km DISPATCH pixel (Figure 2e).

Finally, the 100 m resolution disaggregated soil moisture is estimated as: CDF_{all} or $\text{CDF}_{\text{every}}$

$$sm_{100\text{m},j,t} = sm_{1\text{km},min,i} + (sm_{1\text{km},max,i} - sm_{1\text{km},min,i}) \times F\left(\sigma^{\circ}_{100\text{m},j,t}\right) \tag{14}$$

where $F\left(\sigma^{\circ}_{100\text{m},j,t}\right)$ is the cumulative probability of the backscatter obtained from CDF_{all} or $\text{CDF}_{\text{every}}$.

4. Results

4.1. Data Analysis

Given that the applied approaches differ in considering the spatial and temporal variability of the soil properties, it is necessary to investigate the relevance between the used data (DISPATCH and SAR data) and in situ measurements as an essential step for investigating the use of C-SAR data for disaggregation as well as the performance of each method. Three main aspects are analyzed focusing on: (1) the accuracy of the 1 km DISPATCH product; (2) the sensitivity of backscatter to in situ measurements; and (3) the dependence between backscatter and the 1 km DISPATCH product.

Figure 3 is a graphical evaluation of the 1 km DISPATCH product in comparison to the in situ measurements. The figure shows that some of the 1 km DISPATCH product highly deviates from the measurements causing a wide spread of the matchups among the fitted line. Hence, a relatively weak correlation is detected between the matchups recording a determination coefficient (R^2) of 0.311. The mismatch in the spatial extent between the 1 km resolution DISPATCH product and the localized in situ measurements might explain part of the observed weak correlation. The in situ measurement is based on the dielectric constant estimated within a soil volume of a few squared decimeters, which may not be well representative of the soil moisture at the field scale. By contrast, DISPATCH product presents a soil moisture value integrated over a much larger area (1 km^2), which tends to smooth the soil moisture variability in both space and time. Although the 1 km DISPATCH product highly deviates from the measurements, the associated error of the 1 km DISPATCH product is relatively low (RMSD = 0.033 m^3 m^{-3}. In addition, the calculated overall bias is negligible (0.0003 m^3 m^{-3}).

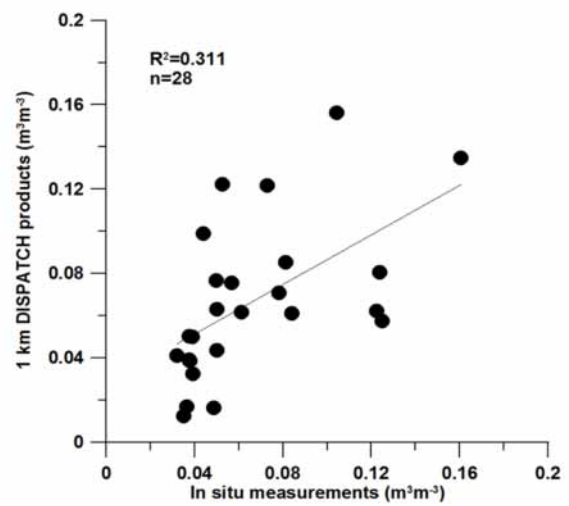

Figure 3. Evaluation of SMOS products (1 km DISPATCH) against the in situ measurements.

Similarly, the sensitivity of the 1 km resolution aggregated backscatter to the in situ measurements is graphically investigated by Figure 4a. The correlation is slightly increased (R^2 = 0.335) in comparison to the correlation detected in Figure 3, indicating that the vertical polarized backscatter could be used for improving the spatial resolution of DISPATCH soil moisture. The spread of the data among the fitted line is lower but has similar pattern to that observed between the 1 km DISPATCH product and the measurements indicating that the spatial scale difference influences the 1 km backscatter and DISPATCH product similarly. Evaluating the sensitivity of the 100 m resolution aggregated backscatter to the in situ measurement (Figure 4b) shows relatively higher R^2 (~0.36). The matchups show high consistency among the fitted line reflecting that the spatial pattern of the moisture content is captured by Sentinel-1 data. The dependence between the backscatter and the 1 km DISPATCH product is also investigated. Figure 5a shows that the 1 km resolution backscatter has a very weak dependence on the 1 km DISPATCH product with R^2 of 0.253 while there is no dependence found between the DISPATCH product and the 100 m resolution backscatter (Figure 5b).

The no dependence between the backscatter and DISPATCH data and the correlation between both data and the in situ measurements confirm that Sentinel-1 data area new source of information by can be used for disaggregation.

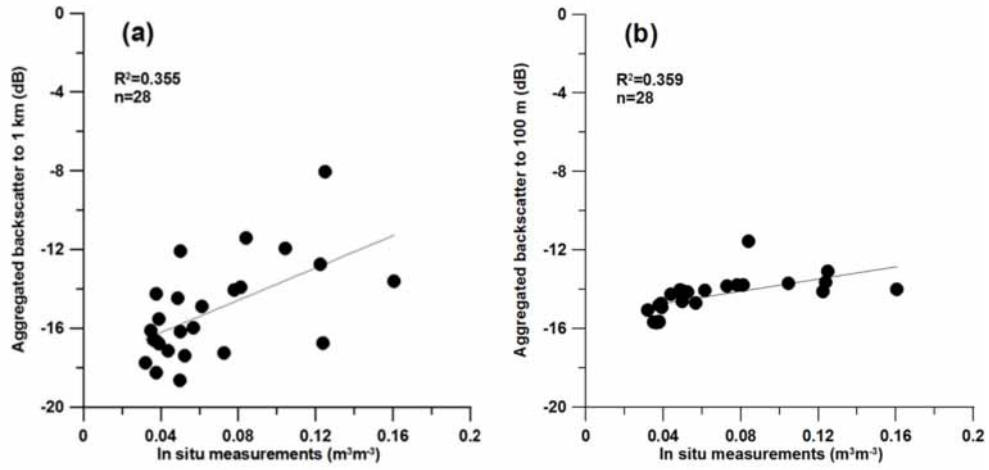

Figure 4. The backscatter aggregated to (**a**) 1 km and to (**b**) 100 m resolutions versus the in situ measurements.

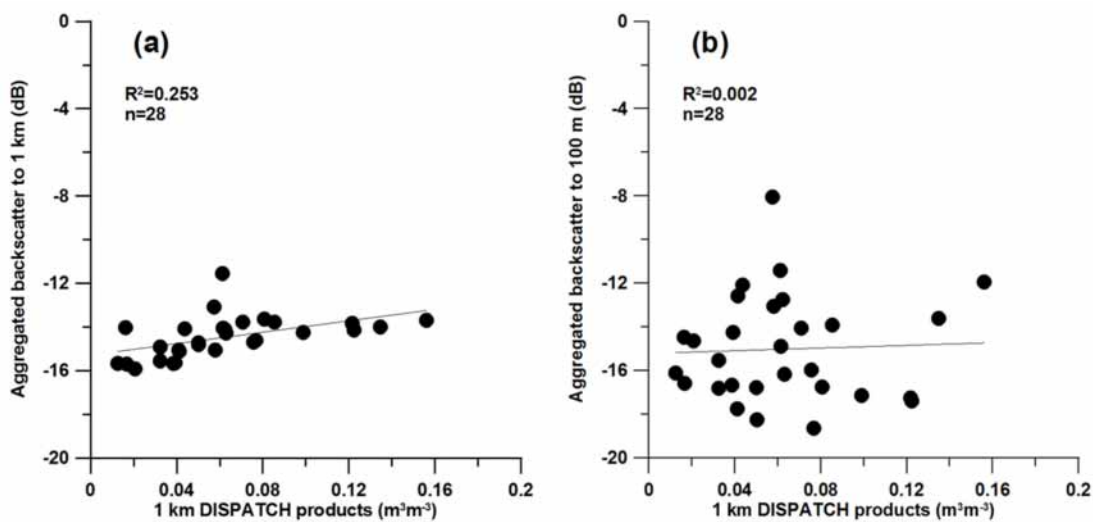

Figure 5. Dependence of the backscatter aggregated to: (**a**) 1 km; and (**b**) 100 m resolutions on the 1 km DISPATCH product.

4.2. Evaluation of Disaggregated Soil Moisture Data Sets

The disaggregated soil moisture obtained from each method is assessed through the comparison with the in situ measurements. The graphical evaluation presented by Figures 6–8 depicts that R^2 values vary across the range 0.292–0.515. Figure 6 shows that the weight method gives the highest R^2 value (0.515) improving the R^2 value resulted from evaluating the 1 km DISPATCH product against the in situ measurements (Figure 3). The spread of the matchups among the fitted line shows that soil moisture are relatively well estimated. However, the figure shows that disaggregated soil moisture corresponding to in situ measurements of ~0.12 m^3 m^{-3} has higher dispersion along *y* axis. The detected dispersion is a direct result of the disaggregation method where the spatial variability of the backscatter (100 m resolution) is the main influencing factor. Both options ($regress_{km}$ and $regress_{100m}$) of the second method are evaluated in Figure 7. The figure shows that $regress_{100m}$ method extremely underestimates soil moisture. This may be due to the averaging of the regression coefficients, which integrate the effects of soil roughness. Indeed, calculating the average over 1 km suppresses the roughness variability from a pixel of 100 m resolution to another leading to an inaccurate representation of the roughness when correlating soil moisture to the backscatter.

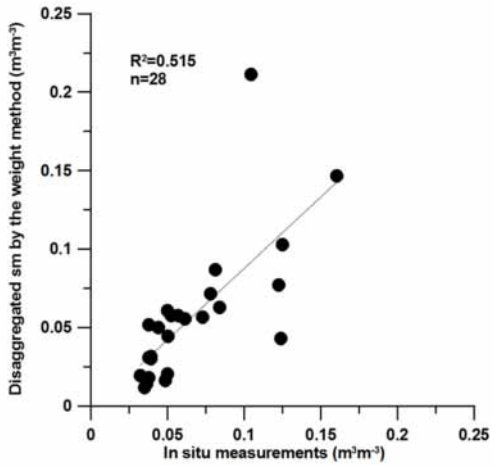

Figure 6. Evaluation of disaggregated soil moisture products by the weight method against the in situ measurements.

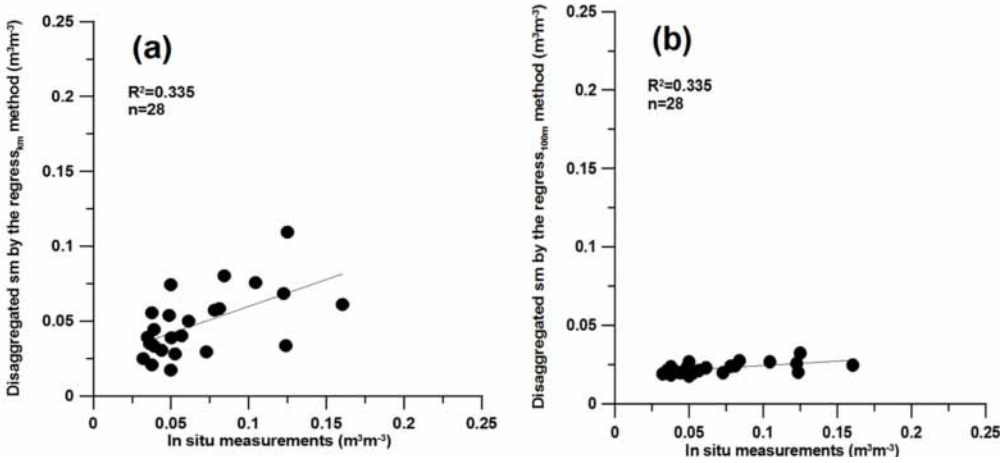

Figure 7. Evaluation of disaggregated soil moisture products by: (**a**) the regress$_{km}$; and (**b**) the regress$_{100m}$ against the in situ measurements.

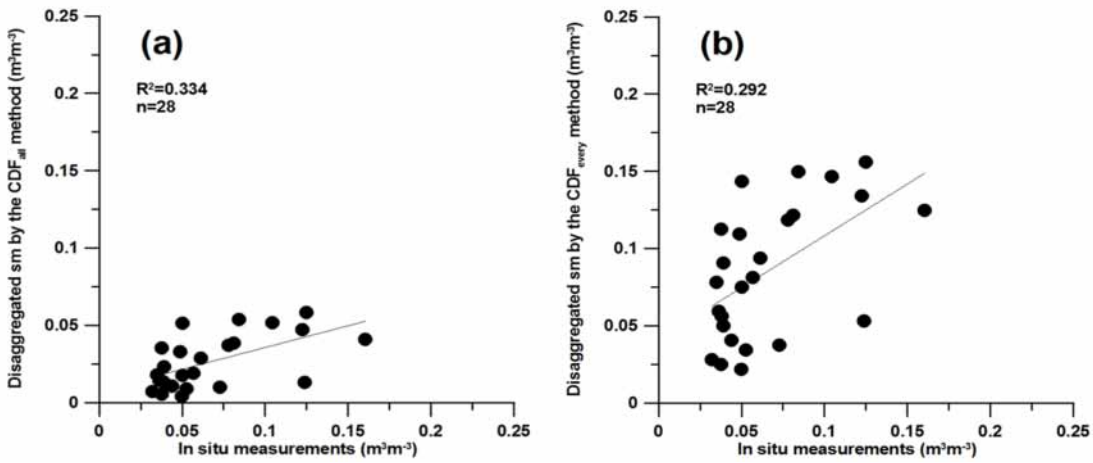

Figure 8. Evaluation of disaggregated soil moisture products by: (**a**) the CDF$_{all}$; and (**b**) the CDF$_{every}$ against the in situ measurements.

The lowest R^2 values are detected from the both options (CDF$_{all}$ and CDF$_{every}$) of the third method recording an R^2 of 0.334 and 0.292, respectively. Figure 8a,b, respectively, shows that the CDF$_{all}$ method gives highly underestimated soil moisture with small range along *y* axis and the CDF$_{every}$ leads to estimates of wide spread with overestimation of soil moisture under the 0.13 m^3 m^{-3} and wider range along *y* axis. This is explained by the number of backscatter used for constructing the cumulative distribution function. In particular, the number of backscatter values affects the ranking process, which is the basis for calculating the cumulative probabilities [42]. In return, the soil moisture range captured by DISPATCH product is disaggregated based on huge number of backscatter in case of the CDF$_{all}$ method while it is disaggregated among much smaller number of backscatter (1/100) in case of the CDF$_{every}$ method.

In addition, the superiority of the weight method to the regress and CDF methods is explained by the nature of the applied algorithm where the weight method depends on the backscatter spatial distribution while the strength of the backscatter–soil moisture relationship controls improvements of the other two methods.

Table 2 listing statistics calculated for quantitatively evaluating the applied methods assures results shown in Figure 6, Figure 7, Figure 8. The weight and regress$_{km}$ methods give the best soil moisture estimates (RMSD of 0.032 m^3 m^{-3} and 0.034 m^3 m^{-3}, respectively). However, the weight approach gives better MAD (Figure 6). The regress$_{km}$ has unstable performance over the study period

where soil moisture is overestimated during dry spells and underestimated during the wet ones. This explains the lower bias obtained from the weight method. Although $regress_{100m}$, CDF_{all} and CDF_{every} give acceptable errors varying across the range 0.042–0.055 m^3 m^{-3}, large MAD and bias are obtained due to the underestimation of soil moisture by the first and the second (Figures 7b and 8a) method, while the third method overestimates soil moisture under the 0.13 m^3 m^{-3} level (Figure 8b).

Table 2. Statistical evaluation of the 1 km DISPATCH product and the applied methods against the in situ measurements.

	R^2	MAD(m^3 m^{-3})	RMSD(m^3 m^{-3})	Bias(m^3 m^{-3})
DISPATCH	0.311	0.025	0.033	0.0003
weight	0.515	0.021	0.032	−0.009
$regress_{km}$	0.335	0.023	0.034	−0.019
$regress_{100m}$	0.335	0.044	0.055	−0.044
CDF_{all}	0.334	0.040	0.049	−0.040
CDF_{every}	0.292	0.036	0.042	0.019

4.3. Temporal and Spatial Pattern

In general, the dry spells occur in summer and fall due to the high evaporative demand with no rainfall. A series of rain events are detected during winter and spring with large temporal variation and various intensities. Maximum and minimum rainfall intensities are observed during the onset and end of May respectively. In this context, Figures 9 and 10 represent the spatial distribution of both the 1 km resolution DISPATCH product and the 100 m resolution disaggregated soil moisture derived from each method over the study area of 5 km^2 shown in Figure 2b. The 1 km DISPATCH product (Figures 9a and 10a) and the weight method results (Figure 9b) perfectly capture the dry and wet conditions of the study period with experienced soil moisture levels reaching 0.3 m^3 m^{-3}. Results of the $regress_{km}$ method show similar temporal pattern with lower moisture levels (0.2 m^3 m^{-3}) during the wet conditions. In contrast, results of the $regress_{100m}$, CDF_{all} and CDF_{every} methods do not represent the soil moisture temporal pattern where maps of $regress_{100m}$ and CDF_{all} correctly represent the dry spells only, while maps of CDF_{every} show high soil moisture during the whole study period.

In addition, all DISPATCH images show that the northern region of the study area is apparently wetter than the southern one. The land use and land cover variation is the main cause of the detected spatial pattern since the DISPATCH algorithm used for producing the 1 km product relies on the evaporative demand along with the relationship between the thermal signature and the land cover. Figure 1b shows that trees are located at the northern region of the study area and at few scattered spots of small areas at the southern east one. Thus, these areas have higher NDVI in comparison to bare soils which represent the highest percentage of the study area [43]. In addition, Figure 1c shows that urban areas are located at the east of the soil moisture station which has different thermal signatures affecting the DISPATCH product. Results of the weight method show the same spatial pattern as for the DISPATCH product (Figure 9b). The weight method gives identical soil moisture levels of both the northern and southern regions representing wet and dry areas, respectively. That is because of the systematic higher backscattering coefficient associated to trees and urban areas located in the northern region in comparison to the southern one. The $regress_{km}$ method gives similar spatial pattern as for the DISPATCH product but with dryer conditions at the northern region (Figure 9c).

Although results of $regress_{100m}$ and CDF_{all} show that the northern region is of relatively higher soil moisture levels than those of the southern one (Figures 9d and 10b), the spatial pattern within each region is not captured. Instead, $regress_{100m}$ leads to a systematic decrement of soil moisture levels from the north to the south direction while CDF_{all} gives higher moisture levels for the southern region compared to those represented by DISPATCH. Furthermore, Figure 10c shows that CDF_{every} leads to similar soil moisture levels over the whole study area to the level represented by the DISPATCH product, but the spatial pattern within both the southern and the northern regions is distorted.

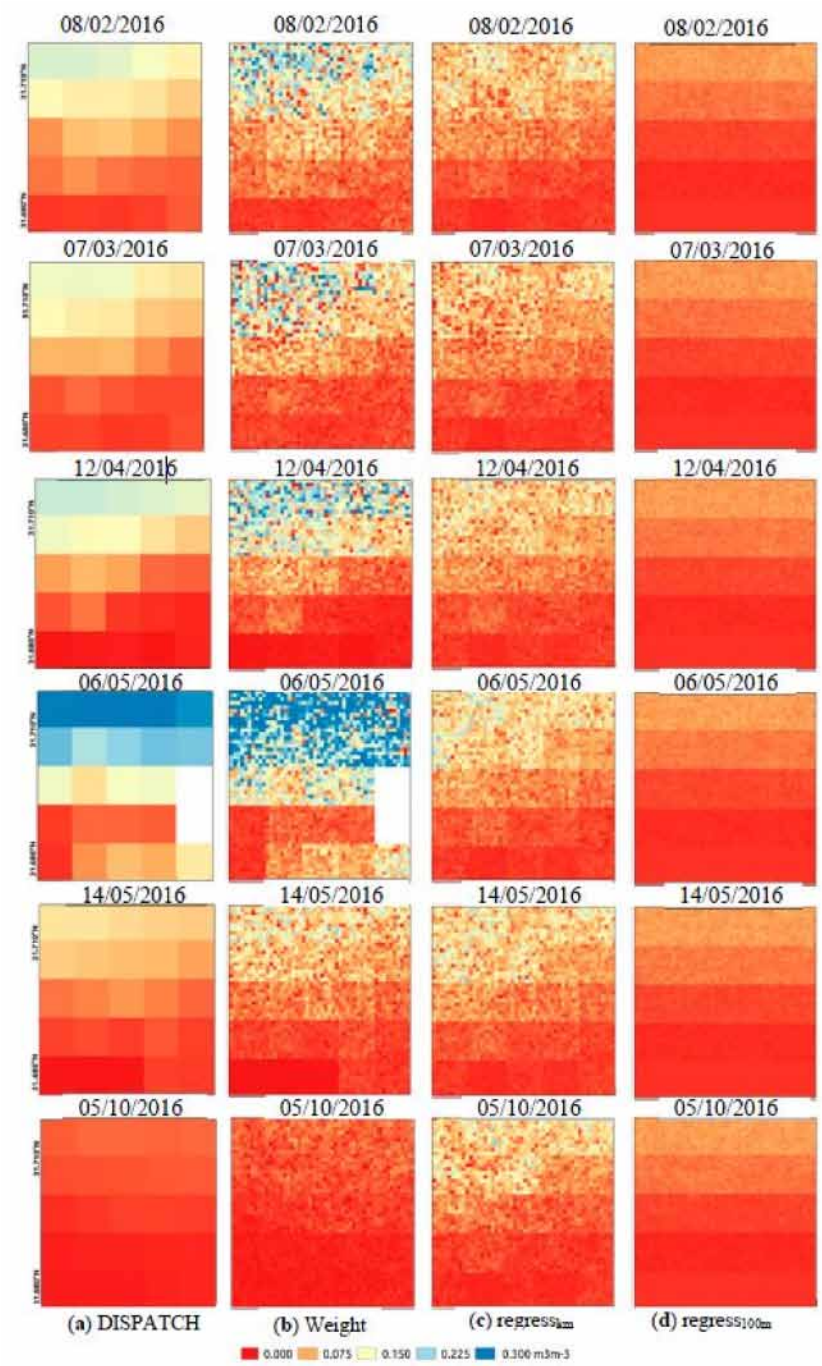

Figure 9. Spatial distribution of the 1 km DISPATCH product and disaggregated soil moisture over of the study area (5 km^2).

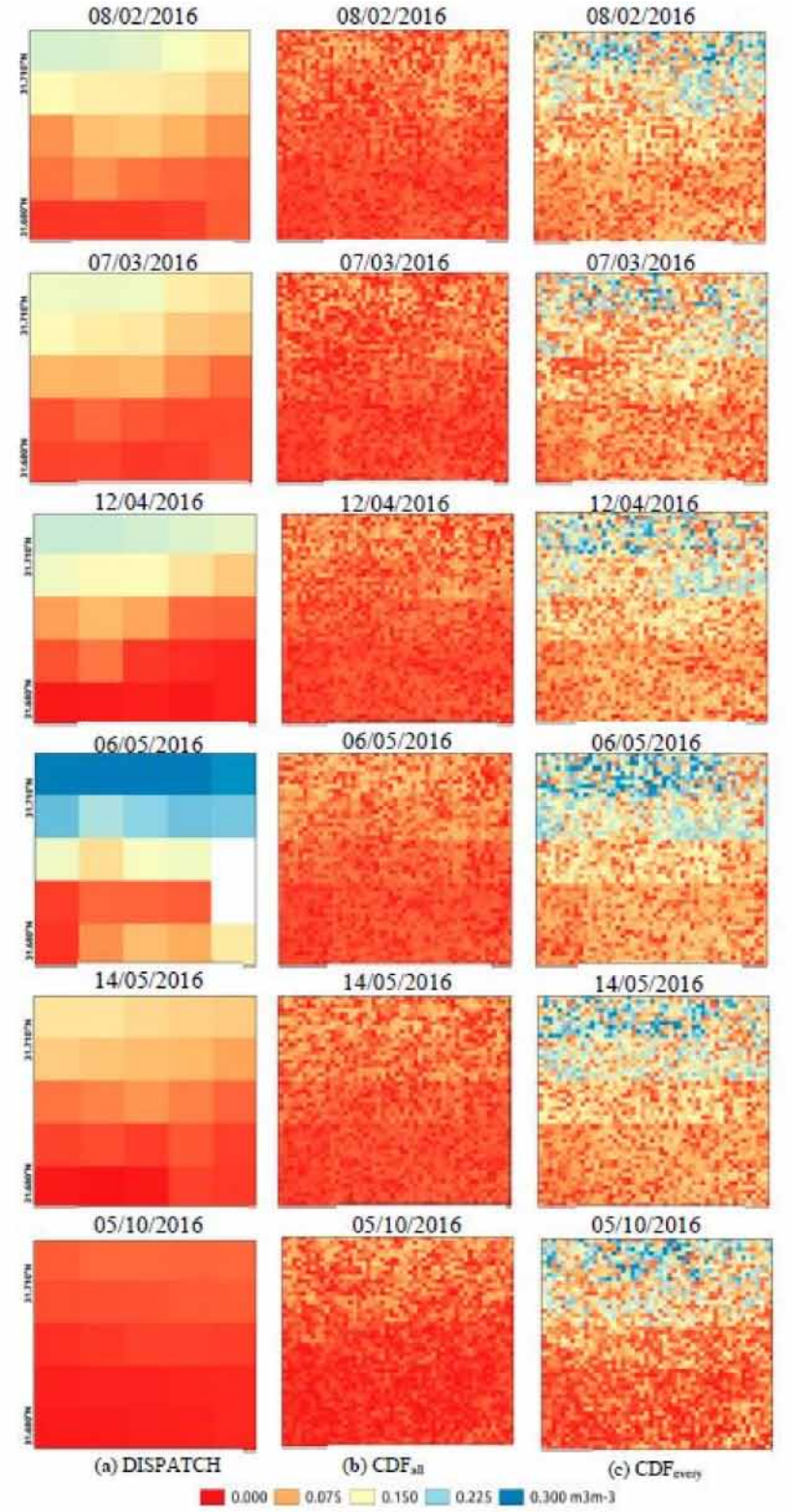

Figure 10. Spatial distribution of the 1 km DISPATCH product and disaggregated soil moisture over of the study area (5 km^2).

4.4. Consistency with DISPATCH Data at the 1 km Resolution

As an inception for analyzing their spatial pattern, the consistency between DISPATCH and 100 m resolution disaggregated products is evaluated. This consistency evaluation is performed over pixels

of the study area representing bare soil conditions only since considering the vegetation contribution to the C-SAR backscatter is not a straight forward operation [31].

Figure 11 is scatter plots comparing between the disaggregated soil moisture by each method and the 1 km DISPATCH products where values of all pixels of all maps; 46 pairs of maps of both disaggregated soil moisture and DISPATCH products are used with excluding those values estimated over vegetated regions. Figure 11a shows that the weight method is the only one that provides disaggregated estimates consistent with the DISPATCH product at all soil moisture levels. That is because the weight method rests on considering the instantaneous spatial variability of the backscatter as indicator for the variability of soil moisture in space. In contrast, estimates of the $\text{regress}_{\text{km}}$ method (Figure 11b) are consistence with the DISPATCH products at soil moisture levels lower than 0.05 m^3 m^{-3} while the consistency distorts at higher levels. In addition, Figure 11c shows that estimates of the $\text{regress}_{\text{100m}}$ have no consistence with the DISPATCH products since the former is of much lower values than the latter. That is attributed to the non-linear relationship between soil moisture and backscatter which does not fully capture the temporal variability of soil moisture. Furthermore, Furthermore, Figure 11d and e show that the CDF method has low consistency with the DISPATCH product especially the $\text{CDF}_{\text{every}}$ which highly overestimates soil moisture. That is because the CDF methods is greatly affected by sm_{min} and sm_{max} which depend on the accuracy of the 1 km DISPATCH product on the particular dates used for estimated *sm* end members, and also by the number of the backscatter values used for calculating the cumulative probabilities.

Table 3 listing the evaluation statistics assessing the concurrence between 100 m resolution disaggregated and DISPATCH products after masking out pixels of vegetated areas assures results of Figure 11. Disaggregated soil moisture of the weight method is the highest correlated to DISPATCH product with the lowest associated error and negligible bias. Much weaker correlation is detected for estimates of the $\text{regress}_{\text{km}}$ and $\text{regress}_{\text{all}}$ with higher associated error and bias while the lowest correlation is observed for estimates of CDF_{all} and $\text{CDF}_{\text{every}}$ with the highest associated error and bias.

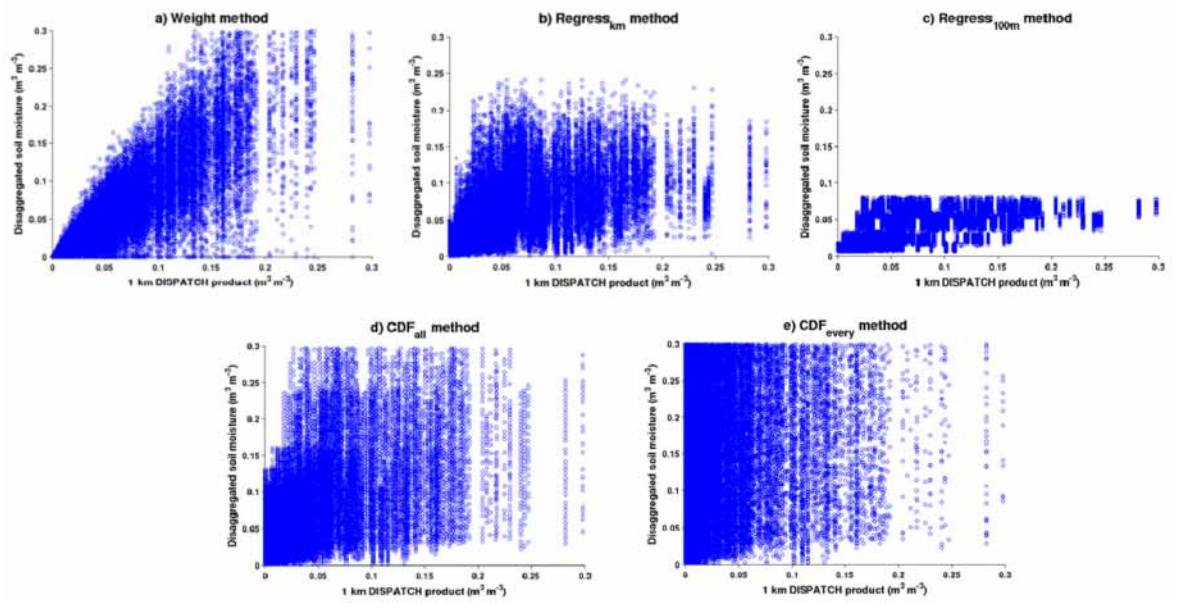

Figure 11. Scatter plots of disaggregated soil moisture (all pixels values of all disaggregated soil moisture maps after masking out values of vegetated areas) produced by: (**a**) weight; (**b**) $\text{regress}_{\text{km}}$; (**c**) regress_{100}; (**d**) CDF_{all}; and (**e**) $\text{CDF}_{\text{every}}$ methods against the corresponding 1 km DISPACTH products

Table 3. Statistical evaluation of the concurrence between 100 m resolution disaggregated and DISPATCH products after masking out pixels of vegetated areas.

	R^2	MAD (m^3 m^{-3})	RMSD (m^3 m^{-3})	Bias (m^3 m^{-3})
weight	0.740	0.017	0.030	−0.0001
$regress_{km}$	0.442	0.030	0.047	−0.0235
$regress_{100m}$	0.337	0.029	0.043	−0.0008
CDF_{all}	0.218	0.054	0.069	0.0368
CDF_{every}	0.159	0.267	0.337	−0.2634

4.5. Spatial Relevancy of Disaggregated Soil Moisture by the Weight Method

The disaggregated soil moisture resulted from the weight method is the best estimates in comparison to other methods results. That is mainly because the weight method distributes soil moisture according to the 100 m to 1 km resolution (aggregated) backscatter ratio.

Thus, nine pixels are selected for investigating the spatial relevancy of the weight method estimates. In particular, the relevancy of disaggregated soil moisture value of the center pixel to those values of the surrounding pixels is investigated. Figure 1c is a Google map image showing the location of the nine pixels and the dominant features. The center pixel; known hereinafter as (1, 1); is selected because: (1) it represents bare soil conditions during the whole study period; (2) it is not affected by any other feature such as building, roads and/or water bodies; and (3) the location of in situ measurements is within this pixel.

Table 4 details the evaluation statistics used for comparison along with the bare soil percentage of each pixel, which show that the relevancy is dependent on the main features existing within each pixel. The higher R^2 (0.650) is detected for pixel (2, 1) with very small RMSE (0.028) where the whole pixel represents bare soils. Similar behavior is detected for pixels (2, 0), (2, 2), (1, 2), and (1, 0). The pixels have lower bare soil percentages (90% > bare soil > 100%) than that detected in pixel (2, 1) because of the roads and small buildings give lower R^2 and RMSD. The effect of buildings and roads clearly appears in pixel (0, 0) and (0, 1) since around 50% and 80% of the two pixels, respectively, represent urban area. Consequently, the spatial patterns shown in maps produced by the weight method are trustworthy (Figure 9b).

Table 4. Evaluation statistics calculated for comparing the disaggregated soil moisture of pixel (1, 1) shown in Figure 1c to the disaggregated soil moisture of the surrounding pixels.

	(0, 0)	(0, 1)	(0, 2)	(1, 0)	(1, 1)	(1, 2)	(2, 0)	(2, 1)	(2, 2)
Bare soil %	40–50	20–30	90–95	>95	100	90–95	>95	100	>95
R^2	0.161	0.045	0.255	0.368	1	0.320	0.484	0.650	0.388
RMSD	0.041	0.062	0.047	0.050	0	0.057	0.044	0.028	0.034
MAD	0.030	0.035	0.032	0.039	0	0.041	0.031	0.020	0.025
Bias	−0.004	0.004	0.001	0.015	0	0.026	0.023	−0.014	−0.001

5. Discussion

A relatively poor correlation is detected between the DISPATCH product and in situ measurements. This is probably due, at least in part, to the mismatch in the spatial extent between the 1 km resolution DISPATCH pixel and the soil moisture probes representative of a tiny soil volume (several squared decimeters). The input datasets used by the DISPATCH algorithm are the main constraints of the spatial and temporal resolution of DISPATCH data. Indeed, the DISPATCH product is obtained from the daily global maps of soil moisture, land surface temperature and vegetation index and its associated parameters over a three-day moving window [29] while the in situ measurements are obtained from the instantaneous measurements of the dielectric constant.

The weight method leads to high improvement in the correlation between *sm* estimates and measurements because of linking *sm* variability in space to the backscatter spatial variability regardless

roughness effect. In fact, the weight method considers no differences of the roughness parameters between the original (1 km) and targeted (100 m) resolution because: (1) the agricultural fields of the study area usually receive the same farming practices and, in addition, no crop was planted during the period of study (due to an unusual lack of precipitation during the months preceding and during the sowing period); and (2) the magnitudes of root mean square height and correlation length vary in very narrow scales (few centimeters and meters respectively) in comparison to the huge areas over which the backscatter is aggregated.

On the other hand, results of the other methods treating the backscatter-*sm* near linear relationship differently [18,19,44] is based mainly on the strength of: (1) backscatter sensitivity to soil moisture; (2) DISPATCH product-backscatter correlation; and (3) DISPATCH product–soil moisture correlation [45]. The backscatter sensitivity to soil moisture is slightly stronger than both the DISPATCH product-backscatter and DISPATCH product–soil moisture correlations (Figures 3–5) indicating that Sentinel-1 data area new source of information. Nonetheless, the 100 m *sm* product resulted from all methods based on the backscatter-*sm* near linear relationship do not show significant improvement.

The spatial and temporal soil moisture patterns provided by the weight method are similar to those of the DISPATCH product. This is due to the fact that the weight method relies on the instantaneous backscatter–soil moisture relationship only, while the other methods are based on the near-linear (temporal) relation between backscatter and soil moisture time series.

6. Conclusions

The 40 km resolution SMOS level 3 product is first disaggregated to 1 km resolution using C4DIS processor, which employs the DISPATCH algorithm and ancillary 1 km resolution MODIS data. Then, different methods are applied for disaggregating the 1 km DISPATCH product to 100 m resolution using Sentinel-1 data as an independent source of information. The methods are identified as weight, $\text{regress}_{\text{km}}$, $\text{regress}_{\text{100m}}$, CDF_{all} and $\text{CDF}_{\text{every}}$ methods, and evaluated against in situ measurements collected between 1 January 2016 and 11 October 2016 over a bare soil site in central Morocco. The first (weight) method focuses on the spatial variability of soil moisture while the second and third ($\text{regress}_{\text{km}}$ and $\text{regress}_{\text{100m}}$) accounts for the soil roughness as constant over time. The fourth and fifth (CDF_{all} and $\text{CDF}_{\text{every}}$) methods are based on employing the cumulative probabilities of the backscatter to calculate soil moisture through building cumulative distribution functions.

Based on the obtained results, we firstly conclude that DISPATCH soil moisture weakly correlates with the in situ measurements, notably due to the spatial scale mismatch between the 1 km resolution DISPATCH pixel and the representativeness scale (several squared decimeters) of in situ sensors, despite the satisfying accuracy of the DISPATCH product (RMSD = 0.033 m^3 m^{-3}). Secondly, C-SAR data are an independent source of information where the backscatter–soil moisture correlation is slightly larger than the DISPATCH product–soil moisture correlation, while the DISPATCH product-backscatter correlation is very low.

Among the applied methods, the weight method leads to superior results preserving the soil moisture spatial and temporal patterns over the study area. Moreover, one significant aspect of the validation exercise is that the correlation between 100 m resolution disaggregated and in situsoil moisture is much improved compared to the 1 km resolution DISPATCH data case, with an associated lower error (RMSD = 0.032 m^3 m^{-3}). That is because the weight method correlates the soil moisture spatial variability to the backscatter spatial variability within the 1 km resolution DISPATCH pixel, regardless of roughness effects. The roughness parameters are assumed to be similar at both the 1 km and 100 m resolution since no farming practice has been undertaken during the study period. The other methods vary in improving/distorting the correlation between remotely sensed and in situ measurements since they depend on the backscatter sensitivity to soil moisture along with the DISPATCH product-backscatter and the DISPATCH product–soil moisture correlations. In general, the $\text{regress}_{\text{km}}$ and $\text{regress}_{\text{100m}}$ slightly improves the correlation (R^2 = 0.335) with a RMSD of 0.034 and 0.055, respectively. Similarly, the CDF_{all} method records a R^2 value of 0.0334 with a RMSD

of 0.040 m^3 m^{-3} while the CDF_{every} method records the lowest R^2 value (0.292) with a RMSD of 0.051 m^3 m^{-3}.

Further efforts should be made in the future to test the applicability of the approach to a larger range of surface conditions including vegetated soils, and soils with various roughness and textural characteristics. In fact, the proposed disaggregation methods are tested during bare soil conditions with insufficient rain intensities for agriculture. Hence, further efforts should be made to investigate the behavior of the applied methods during a year with precipitation that better resembles historical patterns. That is because rain affects significantly change soil roughness through breaking the soil crust in a process known as splash erosion. The regress and CDF methods are generally expected to be highly influenced since they inherently consider soil roughness within the parameters controlling the backscatter–soil moisture relationship. In addition, the backscatter–soil moisture relationship is highly influenced by the vegetation cover which highly contributes to the acquired backscatter.

Acknowledgments: This work is a contribution to the REC project funded by the European Commission Horizon 2020 Programme for Research and Innovation (H2020) in the context of the Marie Skłodowska-Curie Research and Innovation Staff Exchange (RISE) action under grant agreement no: 645642. In addition, this work has been partially funded by a public grant of Ministerio de Economía y Competitividad (DI-14-06587) and AGAUR-Generalitat de Catalunya (DI-2015-058).

Author Contributions: Omar Ali Eweys developed the applied methods. The manuscript was written by Omar Ali Eweys and revised by Olivier Merlin, Maria José Escorihuela, Josep M. Villar, Salah Er-Raki, Lionel Jarlan, Saïd Khabba. Abdelhakim Amazirh processed the data for validating soil moisture products over the study site and Luis Olivera processed and provided the DISPATCH data set.

Conflicts of Interest: The authors declare no conflict of interest.

References

1. Njoku, E.G.; Wilson, W.J.; Yueh, S.H.; Dinardo, S.J.; Li, F.K.; Jackson, T.J.; Lakshmi, V.; Bolten, J. Observations of soil moisture using a passive and active low-frequency microwave airborne sensor during SGP99. *IEEE Trans. Geosci. Remote Sens.* **2002**. [CrossRef]
2. Ulaby, F.T.; Moore, R.K.; Fung, A.K. Microwave remote sensing: Active and passive. In *Radar Remote Sensing and Surface Scattering and Emission Theory*; Addison-Wesley: Reading, MA, USA, 1982; Volume 2.
3. Calvet, J.C.; Wigneron, J.P.; Walker, J.; Karbou, F.; Chanzy, A.; Albergel, C. Sensitivity of Passive Microwave Observations to Soil Moisture and Vegetation Water Content: L-Band to W-Band. *IEEE Trans. Geosci. Remote Sens.* **2011**. [CrossRef]
4. Njoku, E.G.; Entekhabi, D. Passive microwave remote sensing of soil moisture. *J. Hydrol.* **1996**, *184*, 101–129. [CrossRef]
5. Kerr, Y.H.; Waldteufel, P.; Wigneron, J.P.; Delwart, S.; Cabot, F.; Boutin, J.; Escorihuela, M.J.; Font, J.; Reul, N.; Gruhier, C.; et al. The SMOS Mission: New Tool for Monitoring Key Elements ofthe Global Water Cycle. *Proc. IEEE.* **2010**. [CrossRef]
6. Kerr, Y.H.; Waldteufel, P.; Wigneron, J.P.; Martinuzzi, J.; Font, J.; Berger, M. Soil moisture retrieval from space: the Soil Moisture and Ocean Salinity (SMOS) mission. *IEEE Trans. Geosci. Remote Sens.* **2001**. [CrossRef]
7. Bitar, A.A.; Leroux, D.; Kerr, Y.H.; Merlin, O.; Richaume, P.; Sahoo, A.; Wood, E.F. Evaluation of SMOS Soil Moisture Products Over Continental U.S. Using the SCAN/SNOTEL Network. *IEEE Trans. Geosci. Remote Sens.* **2012**, *50*, 1572–1586. [CrossRef]
8. Delwart, S.; Bouzinac, C.; Wursteisen, P.; Berger, M.; Drinkwater, M.; Martin-Neira, M.; Kerr, Y.H. SMOS Validation and the COSMOS Campaigns. *IEEE Trans. Geosci. Remote Sens.* **2008**, *46*, 695–704. [CrossRef]
9. Lievens, H.; Tomer, S.K.; Al Bitar, A.; De Lannoy, G.J.M.; Drusch, M.; Dumedah, G.; Hendricks Franssen, H.-J.; Kerr, Y.H.; Martens, B.; Pan, M.; et al. SMOS soil moisture assimilation for improved hydrologic simulation in the Murray Darling Basin, Australia. *Remote Sens. Environ.* **2015**, *168*, 146–162. [CrossRef]
10. Peng, J.; Loew, A.; Merlin, O.; Verhoest, N.E.C. A review of spatial downscaling of satellite remotely sensed soil moisture. *Rev. Geophys.* **2017**. [CrossRef]
11. Chauhan, N.S.; Le Vine, D.M.; Lang, R.H. Discrete scatter model for microwave radar and radiometer response to corn: Comparison of theory and data. *IEEE Trans. Geosci. Remote Sens.* **1994**. [CrossRef]

12. O'Neill, P.E.; Chauhan, N.S.; Jackson, T.J. Use of active and passive microwave remote sensing for soil moisture estimation through corn. *Int. J. Remote Sens.* **1996**, *17*, 1851–1865. [CrossRef]
13. Famiglietti, J.S.; Devereaux, J.A.; Laymon, C.A.; Tsegaye, T.; Houser, P.R.; Jackson, T.J.; Graham, S.T.; Rodell, M.; Van Oevelen, P.J. Ground-based investigation of soil moisture variability within remote sensing footprints during the Southern Great Plains 1997 (SGP97) Hydrology Experiment. *Water Resour. Res.* **1999**, *35*, 1839–1851. [CrossRef]
14. Grayson, R.B.; Western, A.W. Towards areal estimation of soil water content from point measurements: Time and space stability of mean response. *J. Hydrol.* **1998**, *207*, 68–82. [CrossRef]
15. Famiglietti, J.S.; Ryu, D.; Berg, A.A.; Rodell, M.; Jackson, T.J. Field observations of soil moisture variability across scales. *Water Resour. Res.* **2008**, *44*. [CrossRef]
16. Rodriguez-Iturbe, I.; Vogel, G.K.; Rigon, R.; Entekhabi, D.; Castelli, F.; Rinaldo, A. On the spatial organization of soil moisture fields. *Geophys. Res. Lett.* **1995**, *22*, 2757–2760. [CrossRef]
17. Piles, M.; Entekhabi, D.; Camps, A. A Change Detection Algorithm for Retrieving High-Resolution Soil Moisture From SMAP Radar and Radiometer Observations. *IEEE Trans. Geosci. Remote Sens.* **2009**. [CrossRef]
18. Das, N.N.; Entekhabi, D.; Njoku, E.G. An algorithm for merging SMAP radiometer and radar data for high-resolution soil-moisture retrieval. *IEEE Trans. Geosci. Remote Sens.* **2011**, *49*, 1504–1512. [CrossRef]
19. Das, N.N.; Entekhabi, D.; Njoku, E.G.; Shi, J.J.C.; Johnson, J.T.; Colliander, A. Tests of the SMAP combined radar and radiometer algorithm using airborne field campaign observations and simulated data. *IEEE Trans. Geosci. Remote Sens.* **2014**, *52*, 2018–2028. [CrossRef]
20. Carlson, T. An Overview of the Triangle Method for Estimating Surface Evapotranspiration and Soil Moisture from Satellite Imagery. *Sensors* **2007**, *7*, 1612–1629. [CrossRef]
21. Carlson, T.N.; Gillies, R.R.; Perry, E.M. A method to make use of thermal infrared temperature and NDVI measurements to infer surface soil water content and fractional vegetation cover. *Remote Sens. Rev.* **1994**, *9*, 161–173. [CrossRef]
22. Moran, M.S.; Clarke, T.R.; Inoue, Y.; Vidal, A. Estimating crop water deficit using the relation between surface-air temperature and spectral vegetation index. *Remote Sens. Environ.* **1994**, *49*, 246–263. [CrossRef]
23. Merlin, O.; Escorihuela, M.J.; Mayoral, M.A.; Hagolle, O.; Al Bitar, A.; Kerr, Y. Self-calibrated evaporation-based disaggregation of SMOS soil moisture: An evaluation study at 3 km and 100 m resolution in Catalunya, Spain. *Remote Sens. Environ.* **2013**, *130*, 25–38. [CrossRef]
24. Merlin, O.; Rudiger, C.; Bitar, A.A.; Richaume, P.; Walker, J.P.; Kerr, Y.H. Disaggregation of SMOS Soil Moisture in Southeastern Australia. *IEEE Trans. Geosci. Remote Sens.* **2012**. [CrossRef]
25. Merlin, O.; Al Bitar, A.; Walker, J.P.; Kerr, Y. A sequential model for disaggregating near-surface soil moisture observations using multi-resolution thermal sensors. *Remote Sens. Environ.* **2009**, *113*, 2275–2284. [CrossRef]
26. Lagouarde, J.-P.; Bach, M.; Sobrino, J.A.; Boulet, G.; Briottet, X.; Cherchali, S.; Coudert, B.; Dadou, I.; Dedieu, G.; Gamet, P.; et al. The MISTIGRI thermal infrared project: Scientific objectives and mission specifications. *Int. J. Remote Sens.* **2013**, *34*, 3437–3466. [CrossRef]
27. Köppen Climate Classification. Available online: https://en.wikipedia.org/wiki/K%C3%B6ppen_climate_classification (accessed on 30 October 2017).
28. Merlin, O.; Olivera, L.; Hssaine, B.A.; Amazirh, A.; Rafi, Z.; Ezzahar, J.; Gentine, P.; Khabba, S.; Gascoin, S.; Er-Raki, S. A phenomenological model of soil evaporative efficiency using soil moisture and radiometric temperature data. *Agric. For. Meteorol.* in review.
29. Molero, B.; Merlin, O.; Malbéteau, Y.; Al Bitar, A.; Cabot, F.; Stefan, V.; Kerr, Y.; Bacon, S.; Cosh, M.H.; Bindlish, R.; et al. SMOS disaggregated soil moisture product at 1 km resolution: Processor overview and first validation results. *Remote Sens. Environ.* **2016**, *180*, 361–376. [CrossRef]
30. Merlin, O.; Walker, J.P.; Chehbouni, A.; Kerr, Y. Towards deterministic downscaling of SMOS soil moisture using MODIS derived soil evaporative efficiency. *Remote Sens. Environ.* **2008**, *112*, 3935–3946. [CrossRef]
31. Eweys, O.A.; Elwan, A.A.; Borham, T.I. Retrieving topsoil moisture using RADARSAT-2 data, a novel approach applied at the east of The Netherlands. *J. Hydrol.* **2017**, *555*, 670–682. [CrossRef]
32. Jarlan, L.; Khabba, S.; Er-Raki, S.; Le Page, M.; Hanich, L.; Fakir, Y.; Merlin, O.; Mangiarotti, S.; Gascoin, S.; Ezzahar, J.; et al. Remote Sensing of Water Resources in Semi-Arid Mediterranean Areas: The joint international laboratory TREMA. *Int. J. Remote Sens.* **2015**, *36*, 4879–4917. [CrossRef]
33. International Joint Laboratory. *Remote Sensing and Water Resources in the Semi-Arid Mediterranean*. Available online: http://trema.ucam.ac.ma (accessed on 30 October 2017).

34. Sentinel Application Platform. Available online: http://step.esa.int/main/toolboxes/snap/ (accessed on 30 October 2017).
35. Wagner, W.; Pathe, C.; Doubkova, M.; Sabel, D.; Bartsch, A.; Hasenauer, S.; Blöschl, G.; Scipal, K.; Martínez-Fernández, J.; Löw, A. Temporal Stability of Soil Moisture and Radar Backscatter Observed by the Advanced Synthetic Aperture Radar (ASAR). *Sensors* **2008**, *8*, 1174–1197. [CrossRef] [PubMed]
36. Alvarez-Mozos, J.; Casali, J.; Gonzalez-Audicana, M.; Verhoest, N.E.C. Assessment of the operational applicability of RADARSAT-1 data for surface soil moisture estimation. *IEEE Trans. Geosci. Remote Sens.* **2006**. [CrossRef]
37. Baghdadi, N.; Gherboudj, I.; Zribi, M.; Sahebi, M.; King, C.; Bonn, F. Semi-empirical calibration of the IEM backscattering model using radar images and moisture and roughness field measurements. *Int. J. Remote Sens.* **2004**, *25*, 3593–3623. [CrossRef]
38. Ulaby, F.T.; Moore, R.K.; Fung, A.K. Microwave remote sensing: Active and passive. Volume III: from theory to applications. In *Microwave Remote Sensing: Active and Passive. Volume III: From Theory to Applications*; Remote Sensing Series 4; Artech House: Norwood, MA, USA, 1986.
39. Zribi, M.; Gorrab, A.; Baghdadi, N.; Lili-Chabaane, Z.; Mougenot, B. Influence of radar frequency on the relationship between bare surface soil moisture vertical profile and radar backscatter. *IEEE Geosci. Remote Sens. Lett.* **2014**, *11*, 848–852. [CrossRef]
40. Tomer, S.; Al Bitar, A.; Sekhar, M.; Zribi, M.; Bandyopadhyay, S.; Sreelash, K.; Sharma, A.K.; Corgne, S.; Kerr, Y. Retrieval and Multi-scale Validation of Soil Moisture from Multi-temporal SAR Data in a Semi-Arid Tropical Region. *Remote Sens.* **2015**, *7*, 8128–8153. [CrossRef]
41. Fang, B.; Lakshmi, V. Passive/active microwave soil moisture retrieval disaggregation using SMAPVEX12 data. In Proceedings of the 11th SPIE Asia-Pacific Remote Sensing Symposium, Honolulu, HI, USA, 24–27 September 2018. [CrossRef]
42. Raes, D. *Frequency Analysis of Rainfall Data*; K.U. Leuven Inter-University Programme in Water Resources Engineering (IUPWARE): Leuven, Belgium, 2004; p. 42.
43. Thomsen, L.M.; Baartman, J.E.M.; Barneveld, R.J.; Starkloff, T.; Stolte, J. Soil surface roughness: Comparing old and new measuring methods and application in a soil erosion model. *SOIL* **2015**, *1*, 399–410. [CrossRef]
44. Crow, W.T.; Berg, A.A.; Cosh, M.H.; Loew, A.; Mohanty, B.P.; Panciera, R.; De Rosnay, P.; Ryu, D.; Walker, J.P. Upscaling sparse ground-based soil moisture observations for the validation of coarse-resolution satellite soil moisture products. *Rev. Geophys.* **2012**, *50*. [CrossRef]
45. Velde, R.; Van der Salama, M.S.; Eweys, O.A.; Wen, J.; Wang, Q. Soil Moisture Mapping Using Combined Active/Passive Microwave Observations Over the East of the Netherlands. *IEEE J. Sel. Top. Appl. Earth Obs. Remote Sens.* **2015**. [CrossRef]